Journal of Dermatological Science (2008) 50, 155–158

ELSEVIER

Journal of Dermatological SCIENCE

www.intl.elsevierhealth.com/journals/jods

LETTER TO THE EDITOR

Vitamin D_3 inhibits expression of bullous pemphigoid antigen 1 through post-transcriptional mechanism without new protein synthesis

KEYWORDS
Keratinocyte; Basement membrane zone; Promoter; Gene

Bullous pemphigoid (BP) is the most common autoimmune blistering skin disease, and two autoantigens, BPAG1 (230 kD bullous pemphigoid antigen; BP230) and BPAG2 (180-kD bullous pemphigoid antigen, BP180), have been well characterized [1]. ELISA (enzyme-linked immunosorbent assay) tests for these antigens are now available in clinical practice [2,3]. BPAG1 is a component of hemidesmosomes, which are critical attachment complexes at the cutaneous basement membrane zone, and facilitates the association of keratin intermediate filaments with the hemidesmosomes [4]. Thus, BPAG1 expression can affect the integrity of the cutaneous basement membrane zone and also keratinocyte morphology. Therefore, modulation of BPAG1 expression may have something to do with conditions skin diseases, including BP.

Vitamin D_3 (VD3) was initially known for its role in mineral (calcium and phosphorus) homeostasis and maintenance of normal skeletal structures. It is now clear that VD3 is also involved in cell differentiation, cell proliferation, immune responses and inflammation [5]. In the area of clinical dermatology, topical application of VD3 is widely used for the treatment of psoriasis. Recently, some patients with vitiligo vulgaris and other keratinizing diseases have also been successfully treated using topical VD3. Furthermore, VD3 was given systemically to a great number of patients with osteoporosis, cancers and autoimmune diseases.

Abbreviations: BP, bullous pemphigoid; BPAG, bullous pemphigoid antigen; ELISA, enzyme-linked immunosorbent assay; NHEK, normal human epidermal keratinocytes; VD3, vitamin D_3.

This study examined the effect of VD3 on BPAG1 gene expression. In addition, to investigate the molecular mechanism, we measured the effect of VD3 on changes in promoter activity of the BPAG1 gene.

Normal human epidermal keratinocytes (NHEK) grown under serum-free conditions (Keratinocyte-SFM medium; Invitrogen, Carlsbad, CA) were incubated with $1\alpha,25(OH)_2D3$ (Teijin, Japan) at a concentration of 10^{-8} M for 24 and 48 h. Then total RNA was isolated from cultured NHEK, and BPAG1 mRNA levels were determined by northern blot analysis using a 2.6 kb BPAG1 gene cDNA [6]. As shown in Fig. 1A, incubation of VD3 at 10^{-8} M decreased BPAG1 gene expression. The inhibition rate was more than 70% at both 24- and 48-h incubation times. We also performed RT-PCR analysis using primers for BPAG1 cDNA [7], which gave similar results (data not shown). When keratinocytes were cultured with $1\alpha,25(OH)_2D3$ at several concentrations for 24 h, we found clear inhibition at less than 10^{-12} M of VD3 (Fig. 1B). This study indicates that VD3, even at a relatively low concentration, shows a strong inhibitory effect on BPAG1 gene expression.

To know the effect of VD3 on BPAG1 expression at protein level, we preformed Western blot analysis. NHEK were treated with VD3 at 10^{-8} M for 48 h. The samples were run on SDS-PAGE gels and reacted with anit-human BPAG1 antibody. As shown in Fig. 1C, incubation of VD3 at 10^{-8} M clearly decreased BPAG1 expression at protein level as well as mRNA level.

Next, to examine whether the VD3-elicited downregulation of the BPAG1 gene was dependent on ongoing protein synthesis, similar inhibition studies were performed in the presence and absence of cycloheximide (10 mg/ml). A 24-h incubation of cultured NHEK with VD3 (10^{-8} M) in the absence of cycloheximide resulted in the reduction of BPAG1 mRNA level. Cycloheximide treatment did not alter the inhibition of BPAG1 gene expression by VD3, suggesting that downregulation of BPAG1 gene expression is independent of active protein synthesis (Fig. 2A).

0923-1811/$30.00
doi:10.1016/j.jdermsci.2007.12.003

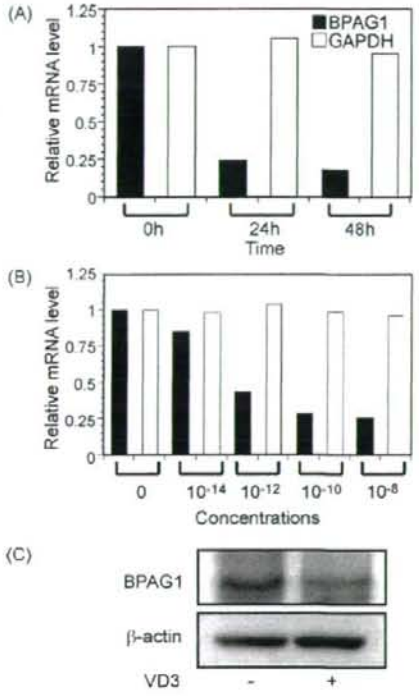

Fig. 1 Effects of VD3 on BPAG1 mRNA expression. Normal human epidermal keratinocytes (NHEK) were cultured routinely using keratinocyte-serum-free medium. (A) Keratinocytes were grown in VD3, $1\alpha,25(OH)^2D3$ at 10^{-8} for 24 and 48 h. After keratinocytes were treated with VD3, total RNA was fractionated on 1.0% agarose gels and transferred to nitrocellulose membranes, which were hybridized with a 2.6-kb BPAG1 gene cDNA and with a 1.3-kb human glyceraldehyde-3-phosphate dehydrogenase (GAPDH) cDNA labeled with ^{32}P. The intensity of the autoradiographic bands was quantified by scanning densitometry. The values were expressed relative to that at 0 h. (■), BPAG1 mRNA; (□), GAPDH mRNA. Data were means of two samples. (B) NHEK cultures were incubated with different concentrations of VD3 (0 M, 10^{-14} M, 10^{-12} M, 10^{-10} M, 10^{-8} M) for 24 h and the BPAG1 mRNA level was then determined by northern blot analysis. The values were expressed relative to that at concentration of 0 M. (■), BPAG1 mRNA; (□), GAPDH mRNA. Data were means of two samples. (C) NHEK were treated with VD3 at 10^{-8} M for 48 h. Total protein from cell cultures was subjected to Western blotting with a anit-human BPAG1 antibody (E-14, Santa Cruz Biotech, Santa Cruz, CA). The samples were run on SDS-PAGE gels, transferred onto nitrocellulose, blocked with 5% non-fat dry milk in TBST and probed with the antibody in TBST overnight at 4 °C. Membrane was further treated with peroxidase-conjugated secondary antibodies (Amersham Pharmacia Biotech, Piscataway, NJ, USA) and developed by ECL (Amersham). Anti-β-actin antibody was used as control.

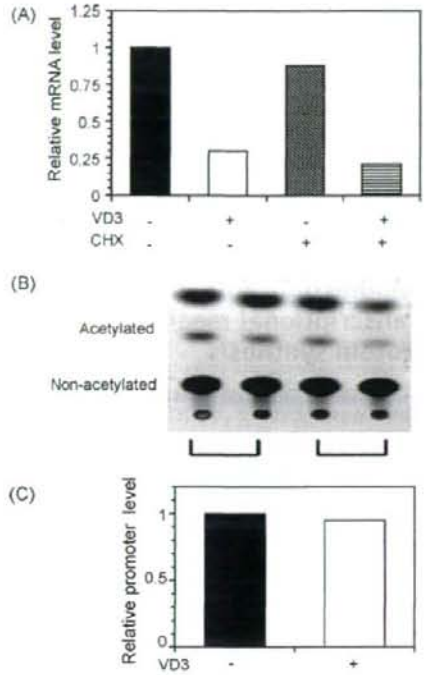

Fig. 2 Mechanisms of inhibitory effects of VD3. (A) NHEK cultures were incubated in the presence (+) or absence (−) of VD3 (10^{-8} M) and/or cycloheximide (CHX; 10 mg/ml) for 24 h. Relative BPAG1 mRNA levels were quantified. The values were expressed relative to that of sample of VD3(−) and CHX(−). Data were means of two samples. (B) The human BPAG1 promoter-DNA/chloramphenicol acetyl transferase (CAT) reporter gene plasmid pBP2.6CAT, containing the BPAG1 promoter region extending from −2600 to −1, was used for transient transfection of cultured NHEK. Transfection was performed with a commercial kit (Dotap; Boehringer Mannheim, Germany), and VD3 (10^{-8} M) was added to cultures. CAT activity in the cell cultures was determined by the incubation of cell extracts with [^{14}C]chloramphenicol followed by the separation of the acetylated and nonacetylated forms by thin-layer chromatography 24 h after transfection. Promoter activity was determined by computing the radioactivity in the acetylated forms of chloramphenicol as a percent of total radioactivity. Data were means of two samples.

We performed transient transfection with BPAG1 promoter reporter gene constructs to investigate the mechanism responsible for VD3-elicited down-regulation of BPAG1 gene expression. Active *cis*-elements conferring keratinocyte-specific expression of the gene have been shown to be present in 2.6 kb of 5′-flanking DNA of the BPAG1 gene [6]. The human BPAG1 promoter-DNA/chloramphenicol acetyl transferase (CAT) reporter gene plasmid was transfected into cultured NHEK and then VD3 (10^{-8} M) was added to the cultures. The CAT activity

in the cell cultures was determined 24 h after transfection. The results showed that the addition of VD3 failed to inhibit the promoter activity of the BPAG1 gene (Fig. 2B). This suggests that the VD3-elicited inhibition of these genes might result from keratinocyte regulatory mechanisms operating at the post-transcriptional level.

In this study, we examined the effect of VD3 on the expression of the BPAG1 in cultured NHEK at mRNA, protein and promoter levels. BPAG1 gene and protein expression was markedly inactivated by VD3 whereas VD3 did not alter the promoter activity of BPAG1. Previously we have shown that TGF-β and IFN-γ inhibit BPAG1 gene expression, but BPAG1 promoter activity is inhibited by IFN-γ, not by TGF-β [6,7]. Thus, VD3 showed an inhibitory effect via a pathway similar to that of TGF-β. One of the previous studies demonstrated that cycloheximide reduced the inhibitory effect of TGF-β1 on BPAG1 mRNA expression, suggesting that newly synthesized proteins were required for BPAG1 regulation by TGF-β [7]. However, the present study showed that cycloheximide treatment did not affect the regulation of the gene by VD3. Collectively, the results show that VD3 may regulate BPAG1 gene expression through post-transcriptional regulation without new protein synthesis. Thus, we demonstrate that the molecular mechanism by which VD3 downregulates BPAG1 gene expression may differ from the mechanisms involved in downregulation by IFN-γ and TGF-β.

In the passive transfer model, rabbit antibodies raised against mouse BPAG2 have been shown to induce BP-like blisters in neonatal mice [8]. Furthermore, direct evidence that BP autoantibodies raised against BPAG2 are pathogenic has been obtained using BPAG2 gene knockout mice rescued by the human ortholog of the gene [9]. These observations indicate that IgG autoantibodies against BPAG2 play a critical role in the pathogenesis of human BP. On the other hand, the role of anti-BPAG1 antibodies in the pathogenesis of BP is still unclear [1]. However, ELISA with recombinant BPAG1 showed high sensitivity and specificity in the sera of BP patients [2]. Moreover, patients with localized BP were shown to have high titers of anti-BPAG1 antibodies and low titers of anti-BPAG2 antibodies, suggesting that the response to BPAG1 maintains the immunological process leading to the chronicity of the disease [10]. Since VD3 and its analogs now were used topically and systemically to many patients [5], we dermatologists should know that modulation of BPAG1 expression by VD3 might provide some advantages or disadvantages in conditions skin diseases, including BP.

Acknowledgements

The authors thanks Ms Yuka Toyomaki and for their skillful technical assistance. This work was supported in part by a Grant-in-Aid of Scientific Research from the Ministry of Education, Culture, Sports, Science and Technology of Japan, and by Kengo-Chan Foundation.

References

[1] Hashimoto T. Skin diseases related to abnormality in desmosomes and hemidesmosomes—editorial review. J Dermatol Sci 1999;20:81–4.
[2] Yoshida M, Hamada T, Amagai M, Hashimoto K, Uehara R, Yamaguchi K, et al. Enzyme-linked immunosorbent assay using bacterial recombinant proteins of human BP230 as a diagnostic tool for bullous pemphigoid. J Dermatol Sci 2006;41:21–30.
[3] Tsuji-Abe Y, Akiyama M, Yamanaka Y, Kikuchi T, Sato-Matsumura KC, Shimizu H. Correlation of clinical severity and ELISA indices for the NC16A domain of BP180 measured using BP180 ELISA kit in bullous pemphigoid. J Dermatol Sci 2005;37:145–9.
[4] Tanaka T, Parry DA, Klaus-Kovtun V, Steinert PM, Stanley JR. Comparison of molecularly cloned bullous pemphigoid antigen to desmoplakin I confirms that they define a new family of cell adhesion junction plaque proteins. J Biol Chem 1991;266:12555–9.
[5] Nagpal S, Lu J, Boehm MF. Vitamin D analogs: mechanism of action and therapeutic applications. Curr Med Chem 2001;8:1661–79.
[6] Tamai K, Li K, Silos S, Rudnicka L, Hashimoto T, Nishikawa T, et al. Interferon-γ-mediated inactivation of transcription of the 230-kDa bullous pemphigoid antigen gene (BPAG1) provides novel insight into keratinocyte differentiation. J Biol Chem 1995;270:392–6.
[7] Ken Harada, Katsuto Tamai, Hajime Nakano, Yamamoto C, Hanada K, et al. Inhibitory effect of TGF-β on expression of 230 kD bullous pemphigoid antigen. Hirosaki Med J 2007;59:7–14.
[8] Liu Z, Diaz LA, Troy JL, Taylor AF, Emery DJ, Fairley JA, et al. A passive transfer model of the organ-specific autoimmune disease, bullous pemphigoid, using antibodies generated against the hemidesmosomal antigen, BP180. J Clin Invest 1993;92:2480–8.
[9] Nishie W, Sawamura D, Goto M, Ito K, Shibaki A, McMillan JR, et al. Humanization of autoantigen. Nat Med 2007;14:378–83.
[10] Kohroh K, Suga Y, Mizuno Y, Ishii N, Hashimoto T, Ikeda S. Case of localized bullous pemphigoid with unique clinical manifestations in the lower legs. J Dermatol 2007;34:482–5.

Chiaki Yamamoto*
Katsuto Tamai
Hajime Nakano
Yasushi Matsuzaki
Takahide Kaneko
Daisuke Sawamura
Department of Dermatology,

Hirosaki University Graduate School of Medicine, Hirosaki, Japan

*Corresponding author at:
Department of Dermatology,
Hirosaki University Graduate School of Medicine,
5 Zaifu-cho, Hirosaki 036-8562,
Aomori, Japan.
Tel.: +81 172 39 5087;
fax: +81 172 37 6060
E-mail address: derma@cc.hirosaki-u.ac.jp
(C. Yamamoto)

31 July 2007

J. Cell. Mol. Med. Vol 12, No 3, 2008 pp. 1-13

Development of a novel antimicrobial peptide, AG-30, with angiogenic properties

Tomoyuki Nishikawa [a], Hironori Nakagami [a, *], Akito Maeda [b], Ryuichi Morishita [c], Nobuhiko Miyazaki [d], Toshihiro Ogawa [d], Yasuhiko Tabata [d], Yasushi Kikuchi [a], Hiroki Hayashi [a], Yoshihiro Tatsu [e], Noboru Yumoto [e], Katsuto Tamai [a], Kazunori Tomono [f], Yasufumi Kaneda [a, *]

[a] *Division of Gene Therapy Science, Graduate School of Medicine, Osaka University, 2-2 Yamada-oka, Suita, Osaka 565-0871, Japan*

[b] *Genomidea, Inc. 7-7-15 Saito Bio-Incubator, Ibaraki, Osaka 567-0085, Japan*

[c] *Division of Clinical Gene Therapy, Graduate School of Medicine, Osaka University, 2-2 Yamada-oka, Suita, Osaka 565-0871, Japan*

[d] *Department of Biomaterials, Institute for Frontier Medical Sciences, Kyoto University, 53 Kawara-cho Shogoin, Sakyo-ku, Kyoto 606-8507, Japan*

[e] *National Institute of Advanced Industrial Science and Technology, Ikeda, Osaka 563-8577, Japan*

[f] *Division of Infection Control and Prevention, Graduate School of Medicine, Osaka University, 2-2 Yamada-oka, Suita, Osaka 565-0871, Japan*

Received: January 11, 2008; Accepted: March 27, 2008

Abstract

The utility of various synthetic peptides has been investigated in clinical trials of the treatment of cancers, infectious diseases and endocrine diseases. In the process of functional gene screening with *in silico* analysis for molecules with angiogenic properties, we generated a small peptide, angiogenic peptide (AG)-30, that possesses both antimicrobial and pro-inflammatory activities. AG-30 has an α-helix structure with a number of hydrophobic or net positively charged amino acids and a propensity to fold into amphipathic structures. Indeed, AG-30 exhibited antimicrobial activity against various bacteria, induced vascular endothelial cell growth and tube formation in a dose-dependent manner and increased neovascularization in a Matrigel plug assay. As a result, AG-30 up-regulated expression of angiogenesis-related cytokines and growth factors for up to 72 hrs in human aortic endothelial cells. To further evaluate the angiogenic effect of AG-30 *in vivo*, we developed a slow-release AG-30 system utilizing biodegradable gelatin microspheres. In the ischaemic mouse hind limb, slow-release AG-30 treatment results in an increase in angiogenic score, an increase in blood flow (as demonstrated by laser Doppler imaging) and an increase in capillary density (as demonstrated by immunostaining with anti-CD31 antibody). These data suggest that the novel peptide, AG-30, may have therapeutic potential for ischaemic diseases.

Keywords: angiogenesis • antimicrobial • peptide • slow release • ischaemic disease

*Correspondence to: Yasufumi KANEDA, M.D., Ph.D., Professor, Division of Gene Therapy Science, Graduate School of Medicine, Osaka University, 2-2 Yamada-oka, Q1 Suita, Osaka 565-0871, Japan.
Tel.: +81-6-6879-3901; Fax: +81-6-6879-3909
E-mail: kaneday@gts.med.osaka-u.ac.jp

and
Hironori NAKAGAMI, M.D., Ph.D,
Assistant Professor, Division of Gene Therapy Science, Graduate School of Medicine, Osaka University.
E-mail: nakagami@gts.med.osaka-u.ac.jp

doi: 10.1111/j.1582-4934.2008.00341.x

Introduction

Advances in analytic techniques have allowed for the characterization of synthetic peptides, and the utility of various synthetic peptides has been investigated in clinical trials of the treatment of cancers, infectious diseases and endocrine diseases. Synthetic peptides have been widely used for clinical trials to treat intractable human diseases such as cancers, infectious diseases and endocrine diseases [1–3]. Unlike retrovirus vectors, synthetic peptides have little chance to integrate or recombinate to host genome, and can be analysed for purity and fidelity of sequencing using well-established analytical techniques [2].

One class of antimicrobial peptides possesses both antimicrobial and proinflammatory activities and can modulate human immune system activity [4–6]. These peptides exhibit potent killing of a broad range of micro-organisms and serve as a first-line defence system as well as interact with host repair and adaptive immune responses [7], and levels of these peptides are increased in the context of inflammation and injury [8, 9]. Major antimicrobial peptides in mammals include the family of defensins and cathelicidin peptides. Antimicrobial peptides of the cathelicidin family consist of an amphipathic a-helix with positive charged residues separate from hydrophobic residues. These structures appear to be critical for the ability of these peptides to interact with the negatively charged microbial membrane in the initiation of antimicrobial effects and may also induce growth and migration of endothelial cells to achieve angiogenesis.

Studies have demonstrated that molecules, PR-39 and LL-37, have potential for the treatment of ischaemic cardiovascular diseases [10, 11]. PR-39 is an anti-microbial peptide of the porcine cathelicidin family and induces angiogenesis by inhibiting the ubiquitin-proteasome-dependent degradation of HIF-1α [10]. The human cathelicidin family molecule, LL-37/hCAP18, is a 37-amino acid peptide beginning with two leucine residues that forms a linear amphipathic α-helix and that possesses a broad spectrum of antimicrobial activity [11]. Further, LL-37/hCAP18 acts as a chemoattractant of neutrophils, monocytes and T cells and promotes angiogenesis by binding to a G-protein-coupled receptor upstream of the PLC-γ/PKC/NFkB, ERK-1 and 2 MAPK, and the PI3K/Akt pathways [12]. Thus, some antimicrobial peptides can also stimulate angiogenesis.

We recently screened a human cDNA library in an attempt to isolate angiogenic factors and successfully identified a powerful and potent angiogenic cDNA clone (p3743) [13]. Further analysis of the angiogenic clone facilitated the identification of a core sequence of EC growth activity. Interestingly, *in silico* analysis showed that the peptide from the core sequence (MLSLIFLHRLKSMRKRLDRKLRLWHRKNYP) was predicted to form an a-helical structure with a high percentage hydrophobic residues, a structure that is characteristic of various antimicrobial peptides [4–6]. Of note, some antimicrobial peptides (*i.e.* LL37 or PR39) may possess pleiotropically hormonal properties (*e.g.* induction of angiogenesis) as well as antibacterial action. Thus, the goal of the present study was to evaluate the potential angiogenic effect of an antimicrobial-like peptide.

Materials and methods

Peptide synthesis and circular dichroism (CD) spectroscopy analysis

Synthetic AG-30 (NH_2 -MLSLIFLHRLKSMRKRLDRKLRLWHRKNYP-COOH) and control peptide (NH_2 - RSLEGTDRFPFVRLKNSRKLEFKDIKGIKR-COOH) were purchased from Peptide Institute, Inc. (Osaka, Japan). Control peptide and LL-37 were synthesized as per a previous report [12] and purchased from SIGMA Genosys (Hokkaido, Japan).

CD data were acquired with Jasco J-820 Spectrophotometer using a 1-mm path length cuvette [14]. Spectra were collected for samples of 50 μM AG-30 and control (Ctrl) peptide in 20 mM phosphate buffer at pH 7.5 and 37°C, with and without 1-mM 2-oleoyl-1-palmitoyl-*sn*-glycero-3- phosphocholine (POPC) or 1 mM 1-palmitoyl-2-oleoyl-*sn*-glycero-3-[phosphor-rac-(1-glycerol)] (sodium salt) (POPG) liposome. POPC and POPG were purchased from SIGMA-ALDRICH (St. Louis, MO, USA) and Avanti Polar Lipids (Alabaster, AL, USA), respectively.

Minimal inhibitory concentration (MIC) assays

MIC assays were conducted as previously described [15]. *P. aeruginosa* (PA) (ATCC27853), *S. aureus* (SA) (ATCC29213) and *E. coli* (EC) (ATCC25922) were grown in Mueller-Hinton broth (MHB) (Becton Dickison and Co., Sparks, MD, USA). Serial twofold dilutions of peptide were

added to 1 ml of medium containing each type of bacteria (PA, SA and EC) at 1×10^5 CFU/ml. The tubes were incubated at 37°C with vigorous shaking for 16 hrs. The MIC was determined as the lowest peptide concentration that prevented visible growth of bacteria.

Cell cultures

HAECs (human aortic endothelial cells) and HASMCs (human aortic smooth muscle cells) (passage 3) were purchased from Clonetics Corp. (Palo Alto, CA, USA) and were maintained in endothelial basal medium (EBM-2 medium) supplemented with 5% fetal bovine serum (FBS) and endothelial growth supplement, as described previously [16] or smooth muscle medium supplemented with 5% FBS and smooth muscle growth supplement.

Cell viability and migration assay

HAECs and HASMCs (10^3 cells/well) were seeded on 96-well collagen I-coated plates the day before transfection. Cell viability of HAECs and HASMCs were measured using the MTS [3-(4,5-dimethylthiazol-2-yl)-5-(3-carboxymethoxyphenyl)-2-(4-sulfophenyl)-2H-tetrazolium] Assay. On the first, second and fourth day (fifth day for HASMCs) after transfection, 10 μl of CellTiter 96 One Solution Reagent (Promega, Madison, WI, USA) was added to each well, and absorbance at 490 nm was measured.

HAEC chemokinetic migration was assayed using a modified Boyden chamber, as previously described [17]. 10^6 cells/ml of HAEC suspended in 50-μl EBM2 medium containing either AG-30, LL-37 or control peptide (10 μg/ml) were added to the upper chamber. After 24-hr incubation, the membrane was removed. The cells on the lower side of the membrane were stained with Diff-Quick (Sysmex, Hyogo, Japan). The number of cells was counted in eight randomly chosen fields under ×100 magnification.

Chemotactic migration of HAEC in response to AG-30 was also assessed using a modified Boyden chamber as previously described [18]. In brief, AG-30 was added in different concentrations (0.1, 1.0 and 10 μg/ml) in the lower chambers, and HAEC (10^6 cells/ml in 50 μl) suspended in EBM2 medium (1% BSA and no growth factor added) were added to the upper chambers. After 4-hr incubation, the membrane was removed and the migrated cells were counted as described above.

Tube formation assay

HAEC tube formation assay was conducted in triplicate in a 24-well plate using an Angiogenesis Kit (Kurabo, Osaka, Japan), as per the manufacturer's instructions. Human endothelial and fibroblast cells in the kit were cultured in Optimized Medium supplemented with 1% FBS, followed by daily treatment with AG-30 peptide (0.1, 1, 10 μg/ml), LL-37 peptide (1 and 10 μg/ml) or control peptide (1, 10 μg/ml). Seven days later, cells were stained with anti-human CD31 monoclonal antibody. Stained cells were photographed, and tubule-like structures in the images were analysed by an Angiogenesis Image Analyzer (Kurabo, Osaka, Japan).

In vivo Matrigel plug assay

Two different types of Matrigel plug assays were performed as previously described [17]. First, growth factor-depleted Matrigel (0.5 ml, BD Biosciences, Franklin Lakes, NJ, USA) was mixed with 40 U/ml of heparin (Aventis Pharma, Tokyo, Japan) and either AG-30 peptide (10 μg/ml), control peptide (10 μg/ml) or no peptide. The mixture was then injected subcutaneously into C57BL/6 male mice obtained from Oriental Bio Science Co., Ltd. (Kyoto Japan). After 7 days, the mice were humanely killed, and the plugs were recovered and fixed in methanol. For immunostaining, sections were incubated with monoclonal anti-CD31 (PECAM-1) antibody (1:100 dilution, BD Pharmigen, San Diego, CA, USA) and anti-α-smooth muscle actin antibody (1:400 dilution, SIGMA, Saint Louis, MO, USA) overnight at 4°C, and then incubated in Alexa Flour 488 and 546 secondary antibodies (1:500, Molecular Probes, Eugene, OR, USA) for 2 hrs before photography. Next, the directed *in vitro* angiogenesis assay (DIVAA) (Trevigen, Inc., Gaithersburg, MD, USA) was performed essentially as per the manufacture's instructions. In brief, sterilized DIVAA angioreactors were filled with 18 μl of Basement Membrane Extract (BME) with AG-30 peptide (10 μg/ml) or control peptide (10 μg/ml). The angioreactors were implanted subcutaneously into the dorsal area of C57BL/6 male mice (6 weeks of age) and maintained for 15 days. All experimental protocols were approved by the Osaka University Graduate School of Medicine Standing Committee on Animals.

Microarray analysis

HAEC RNA samples that had been stimulated with or without AG-30 peptide (10 μg/ml) after 24 and 72 hrs were extracted, and the quality of these samples was examined using the Agilient 2100 Bioanalyzer (Agilient Technologies, Palo Alto, CA, USA). RNA amplification and labelling was performed following the LRIFLA protocol (Agilent Low RNA Input Fluorescent Linear Amplification Kit Protocol, version 2.0. Agilient Technologies, Palo Alto, CA, USA). AG-30 stimulated and non-stimulated cDNA samples were

labelled by Cyanine 3- and 5-labelled CTP (cystidine 5-triphosphate), respectively. Hybridization was performed according to instructions provided by the Agilent oligonucleotide microarray hybridization user manual (Agilent Technologies, Palo Alto, CA, USA). Finally, 0.75 μg of labelled cDNA was applied to a Whole Human Genome Oligonucleotide Microarray and then hybridized. The arrays were scanned by the Agilent dual-laser DNA microarray scanner and analysed by Feature Extraction software.

Real-time quantitative reverse transcription polymerase chain reaction (qRT-PCR)

After treatment with AG-30 peptide (10 μg/ml), HAEC RNA was extracted at 72-hr time points using the RNeasy Mini kit (QIAGEN, Valencia, CA, USA). Complementary DNA was synthesized using the Thermo Script RT-PCR System (Invitrogen, Carlsbad, CA, USA). Relative gene copy numbers of interleukin-8 (IL-8: Hs00174103), angiopoietin-2 (Ang-2: Hs00169867), Jagged 1 (Jag-1:Hs00164982), insulin-like growth factor-1 (IGF-1: Hs00153126), vascular endothelial growth factor (VEGF: Hs00173626) and GAPDH (Hs99999905) were quantified by real-time qRT-PCR using TaqMan Gene Expression Assays (Applied Biosystems, Foster City, CA, USA). The absolute number of gene copies was normalized using GAPDH and standardized by a sample standard curve. Results are expressed as fold-increase relative to the non-stimulants for copy numbers of each mRNA.

Preparation of gelatin microspheres incorporating AG-30

The carboxyl groups of gelatin with an isoelectric point of 5.0 (MW 100,000) were prepared from pig skin by an acid process (Nitta gelatin Inc., Osaka, Japan) and were chemically converted by introducing amino groups for cationization of gelatin as previously described [19]. To impregnate AG-30 into gelatin microspheres, 20 μl of PBS containing 100 or 500 μg of AG-30 or control peptide was placed onto 2 mg of freeze-dried gelatin microspheres, followed by incubation for 24 hrs at 4°C. Before injection into the ischaemic hindlimb, 80 μl of PBS was added to this solution.

Evaluation of *in vivo* degradation of gelatin microspheres

Gelatin microspheres were radioiodinated using [^{125}I] Bolton-Hunter reagent [20]. The ^{125}I-labelled gelatin microspheres (2 mg/200 1 PBS/mouse) were subcutaneously injected into the back of 6- to 8-week-old C57BL/6 mice (Japan SLC, Inc., Hamamatsu, Japan). At 3, 7, 14 and 21 days after injection, the mouse skin and muscle containing the gelatin microspheres were excised in order to measure their radioactivity on a gamma counter. The radioactivity ratio of the sample to the gelatin microspheres injected initially was measured to express the percentage of remaining radioactivity in the gelatin microspheres. AG-30 was also radioiodinated and gelatin microspheres incorporating 100 μg of ^{125}I-labelled AG-30 were prepared similarly and subcutaneously injected to mice at the injection volume of 200 μl. The percentage of remaining radioactivity in AG-30 was similarly calculated. All animal experiments were performed in accordance with the Institutional Guidelines of Kyoto University on Animal Experimentation.

Mouse hind limb ischaemic model and evaluation of angiogenesis

Wild-type C57Bl/6J mice (8-week old, male) were anaesthetized with ketamine chloride (80 mg/kg) and xyladine sulfate (8 mg/kg) subcutaneously, and unilateral hind limb ischaemia was induced as described previously [21]. The solution containing AG-30 or control peptide was carefully injected into the mouse ischaemic limb with a 26-gauge needle. Three separate injections of cells (intramuscularly into the ischaemic limb, near both the proximal and distal arterial stumps) were performed. All experimental protocols were approved by the Medicine Standing Committee on Animals of the Osaka University Graduate School.

Blood flow was assessed by laser Doppler imaging (LDI: Moor Instruments, Devon, United Kingdom) before and on post-treatment days 7, 14, 21 and 28 as described previously [21]. Mice were assigned to one of four groups: injection of AG-30 (500 μg) with gelatin, AG-30 (100 μg) with gelatin, control peptide (500 μg) with gelatin and only AG-30 (500 μg). Capillary density within the ischaemic thigh adductor skeletal muscles was analysed to obtain specific evidence of vascularity at the level of the microcirculation. After fixation in cold acetone (–20°C for 15 min.), capillary endothelial cells (EC) were identified by immunohistochemical staining with anti-mouse PECAM mAb (Pharmingen, San Diego, CA, USA).

Statistical analysis

All values are expressed as mean ± S.E.M. Analysis of variance with subsequent Fisher's PLSD test was employed to determine the significance of differences in multiple comparisons.

Results

Novel angiogenic peptide, AG-30

Review of the protein databases (Blast in the NCBI database) failed to identify any known proteins with homology to this antimicrobial-like peptide, which we subsequently designated as AG (angiogenic peptide)-30. Structural analysis by the AGADIR program suggested that AG-30 forms an a-helix structure (predicted value: 21.17%) and an amphipathic structure in which most positively charged amino acids are localized to one side of the molecule with most hydrophobic amino acids localized to the other side of the molecule (see hydrophobic cluster analysis [HCA] plot [22] in Fig. 1A). To follow and give a better impression of the environment of each amino acid widely separated by the unfolding of the cylinder, hydrophobic residues were encircled, demonstrating sets of adjacent hydrophobic residues in hydrophobic clusters (Fig. 1B). Of note, there were very few proline or glycine residues that would otherwise interrupt the α-helical structure. The structure of this peptide is reminiscent of that of some antimicrobial peptides that directly interact with bacterial membranes.

Antimicrobial effect of AG-30

To examine whether AG-30 may form a helix structure, CD analysis was performed. AG-30 and the control peptide were subjected to structural analysis in phosphate buffer (PB), and no helical structure was observed for either AG-30 or the control peptide. Importantly, after the addition of POPC liposomes (mimicking a zwitterionic eucaryotic membrane) or POPG liposomes (mimicking a bacterial membrane) in PBS, AG-30 showed a helical propensity in membrane mimetic solvent, especially in POPG. Upon combining AG-30 and liposomes, the negative molar ellipticy, suggestive of a coiled shape, changed to a recognizable positive value, indicative of a helical structure in the region of 185–195 nm (Fig. 1C). The region from 195 to 225 nm also retained a characteristic shape for a coil without liposomes and a helical structure in POPG.

AG-30 showed antimicrobial activity against *P. aeruginosa* (MIC: 5 μg/ml), *E. coli* (MIC: 40 μg/ml), and *S. aureus* (MIC: 20 μg/ml) (Table 1) through a 'lytic' action by attaching to cationic peptides. Addition of exogenous $CaCl_2$ or $MgCl_2$ (3 mmol/L or 6 mmol/L) completely attenuated the antimicrobial effect of AG-30 against *P. aeruginosa* (data not shown). These results suggest that AG-30 transforms its structure to α-helix when it encounters bacterial membrane, thereby acting as antimicrobial peptide by disrupting the bacterial membrane.

Angiogenic property of AG-30

Some antibacterial peptides also possess angiogenic properties. In a human endothelial cell viability assay, AG-30 increased MTS activity in a dose-dependent (from 0.1 to 1.0 μg/ml) manner, and was more potent than LL-37 (Fig. 2A). Treatment with AG-30 also increased vascular smooth muscle cell viability in a dose-dependent manner (from 0.1 to 1.0 μg/ml), as assessed by MTS assay (Fig. 2B). Human cell lines, such as HEK293, SAS (tongue cancer), HuH7 (hepatoma) and HeLa (cervical cancer) did not show significant response in viability in response to AG-30 stimulation (data not shown). In addition, chemokinetic cell migration significantly increased in response to AG-30 (which was more potent than LL-37) but not in response to control peptide (Fig. 2C). We have also addressed the chamotactic action of AG-30 by the addition of AG-30 in the lower chambers and HAEC in the upper chambers. As a result, the treatment of AG-30 with HAEC showed not only chemokinetic migration but also chemotactic action (Fig. 2D), although the chemokinetic action of AG-30 was stronger than chemotactic action. Further, tube formation was greater in response to AG-30 treatment when compared with LL-37 or control peptide treatment (Fig. 2E). These data demonstrate that AG-30 was superior to LL-37 in terms of inducing endothelial cell growth, migration and tube formation.

The *in vivo* angiogenic activity of AG-30 has been evaluated by an established mouse Matrigel plug assay [23]. Matrigel, containing either control peptide or AG-30, was subcutaneously injected into male C57BL/6 mice. Seven days later, neovessels containing intact red blood cells were more numerous in mice that received Matrigel plug containing AG-30 than in mice receiving Matrigel plug containing control peptide. The increased presence of neovessels in the AG-30-treated group relative to the other groups

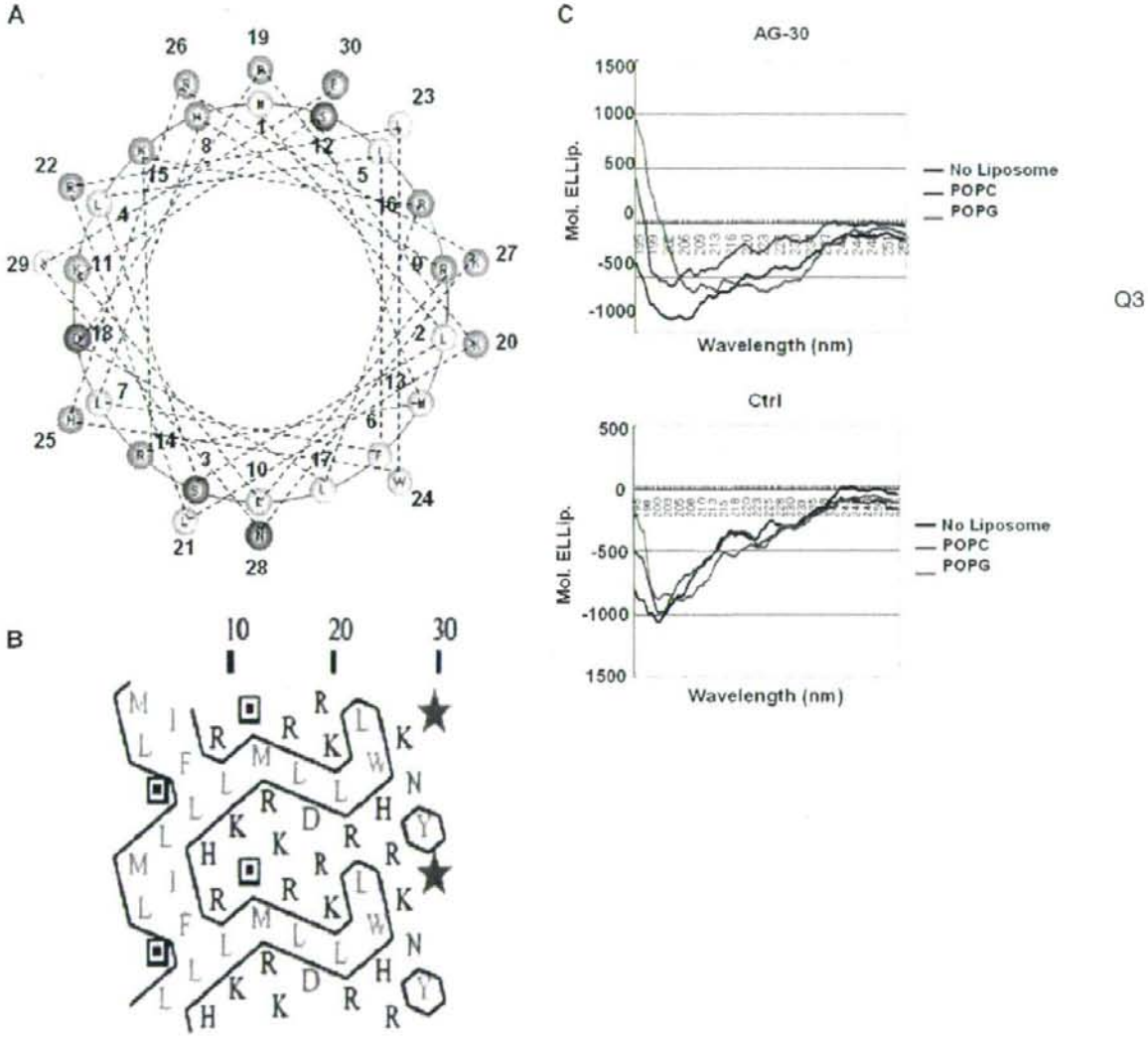

Q3

Fig. 1 Conformation analysis of AG-30. (**A**) Schematic wheel plot of amino acid distribution of AG-30 in alpha-helical structure (http://www-nmr.cabm.rutgers.edu/bioinformatics/Proteomic_tools/Helical_wheel/). The hydrophobic amino acids are represented in gold, positive charged amino acids in green, negative charged amino acids in red-purple, proline in red and the other amino acids in blue-purple. (**B**) Protein sequence analysis on an alpha-helical 2D pattern using an HCA plot (http://bioserv.rpbs.jussieu.fr/RPBS/cgi-bin/Ressource.cgi?chznlg=fr&chzn_rsrc=HCA).The hydrophobic residues are represented in yellow-green and encircled, and different symbols used for P (*), and S (◙). The positively charged amino acids are represented in purple, and the negatively charged amino acid (D) or other amino acids (N) are represented in red. (**C**) Secondary structure analysis of AG-30 and control peptide (Ctrl) by circular dichroism spectroscopy. CD spectra of AG-30 (50 μmol/L) and control peptide (50 μmol/L) without liposome (black line), with POPC (blue line) and with POPG (red line). Molar ellipticities, which indicates dimensions degrees decilitres mol^{-1} $decimeter^{-1}$, were plotted against wavelength from 195 to 255 nm.

	AG30	LL37	Control
E. coli (ATCC 25922)	40.0	5.00	>80
P. aeruginosa (ATCC 27853)	5.00	2.50	>10
S. aureus (ATCC 29213)	20.0	>80	>80

*MIC was defined as the lowest concentration of peptide that inhibited the bacterial visible growth after incubation for 16 hrs at 37°C with vigorous shaking.

was confirmed by immunostaining with anti-CD31 and anti-a-smooth muscle actin antibody (Fig. 3A). Further, these results were reproduced using another type of matrigel assay (DIVAA), and quantification by FITC-lectin staining showed that treatment with AG-30 significantly increased neovessels with a potency that was superior to that of LL-37 (Fig. 3B). In combination with the results demonstrated above, these data suggest that AG-30 induces angiogenesis *via* increased endothelial cell and smooth muscle cell migration and invasion.

Microarray and real-time PCR Analysis in AG-30-treated endothelial cells

To confirm the mechanism of AG-30-induced angiogenesis, differences in gene expression were assessed by microarray analysis (total 43,941 genes). At 6, 24 and 72 hrs after the start of treatment, 47 genes (0.001%), 61 genes (0.13%) and 287 genes (0.65%) were up-regulated and 2 genes (0.00005%), 297 genes (0.67%) and 288 genes (0.66%), were down-regulated, respectively. Subsequent cluster analysis with GeneSpring software revealed at least a twofold increase in angiopoietin 2 (Ang-2), IL8, JAG1, IGF-1, ETS variant gene 7, and chemokine ligand 2 (CCL2) and chemokine receptor 4 (CXCR4) (data not shown). Further, up-regulation of these angiogenesis-related genes occurred in a time-dependent manner for most genes and was maintained for at least 72 hrs (Table 2). We further carried out quantitative RT-PCR of these angiogenesis-related molecules in triplicates to confirm if they would be up-regulated or not. Indeed, we confirmed the increased expression of Ang-2 by 6.24-fold increases in average, IL-8 by 8.45-fold, Jag-1 by 2.82-fold, VEGF by 3.28-fold and IGF-1 by 2.82-fold, respectively, at 72 hrs after AG-30 stimulation (Fig. 4). These results suggest that these angiogenesis-related genes are actually up-regulated and may synergistically induce angiogenesis after the treatment with AG-30.

Effect of slow-release AG-30 in a mouse ischaemic hind limb model

Finally, we evaluated the angiogenic effect of AG-30 in a mouse ischaemic hind limb model. To achieve sustained administration of AG-30 over a local area, a slow-release system was developed using cationic microspheres. As AG-30 includes a number of cationic amino acids, an anionic gelatin might be suitable for slow release of AG-30. However, a part of the gelatin might bind to AG-30 and interfere with its angiogenic effect. Thus, we used PI (isoelectric point) = 5 gelatin, which has been used for the delivery of recombinant FGF-2 in clinical trials of therapeutic angiogenesis. Characterization of the slow release profile of AG-30 (Fig. 5A) revealed that the PI = 5 gelatin slowly dissolved and disappeared in mice within approximately 14 days and that AG-30 was rapidly released within the first 3 days.

At 10 days after unilateral ligation of the femoral artery of the mouse hind limb, blood flow was measured by LDI. Figure 5B shows representative LDI images of hind limb blood flow at 0, 14 and 28 days after injection. Although serial LDI examination revealed natural recovery of hind limb blood flow in the control peptide group, injection of AG-30 (500 μg) with gelatin resulted in more rapid recovery of the ratio of ischaemic(normal blood flow and a significantly sustained increase, but injection of AG-30

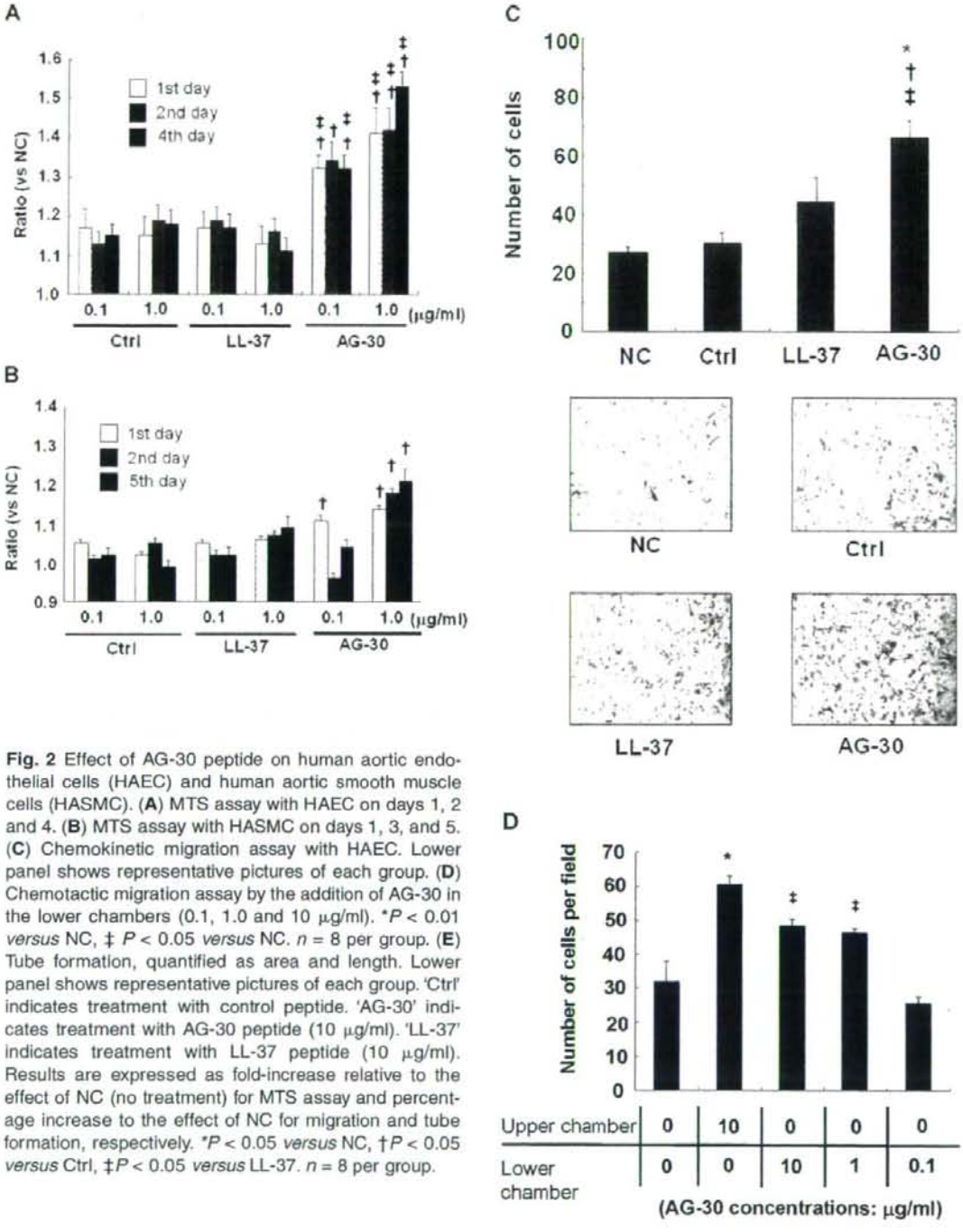

Fig. 2 Effect of AG-30 peptide on human aortic endothelial cells (HAEC) and human aortic smooth muscle cells (HASMC). (**A**) MTS assay with HAEC on days 1, 2 and 4. (**B**) MTS assay with HASMC on days 1, 3, and 5. (**C**) Chemokinetic migration assay with HAEC. Lower panel shows representative pictures of each group. (**D**) Chemotactic migration assay by the addition of AG-30 in the lower chambers (0.1, 1.0 and 10 μg/ml). *$P < 0.01$ *versus* NC, ‡ $P < 0.05$ *versus* NC. $n = 8$ per group. (**E**) Tube formation, quantified as area and length. Lower panel shows representative pictures of each group. 'Ctrl' indicates treatment with control peptide. 'AG-30' indicates treatment with AG-30 peptide (10 μg/ml). 'LL-37' indicates treatment with LL-37 peptide (10 μg/ml). Results are expressed as fold-increase relative to the effect of NC (no treatment) for MTS assay and percentage increase to the effect of NC for migration and tube formation, respectively. *$P < 0.05$ *versus* NC, †$P < 0.05$ *versus* Ctrl, ‡$P < 0.05$ *versus* LL-37. $n = 8$ per group.

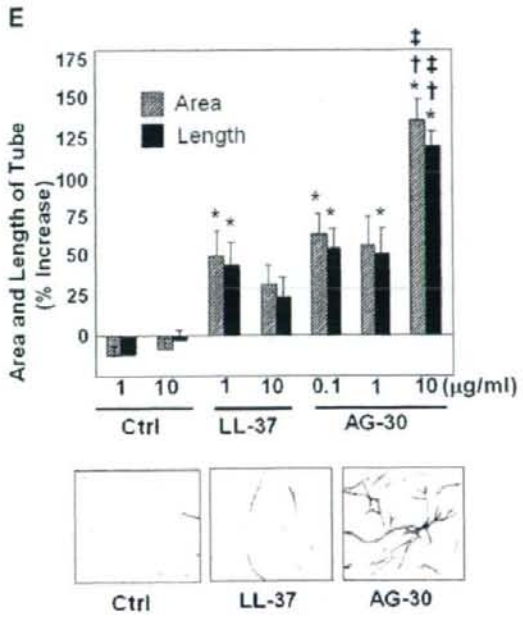

Fig. 2 Continued

(100 μg) with gelatin or only AG-30 did not.

Figure 5C shows representative photomicrographs of tissue immunostained with anti-CD31 antibody. Quantitative analysis revealed that the capillary density was significantly increased in the AG-30 (500 μg) with gelatin group when compared with other groups.

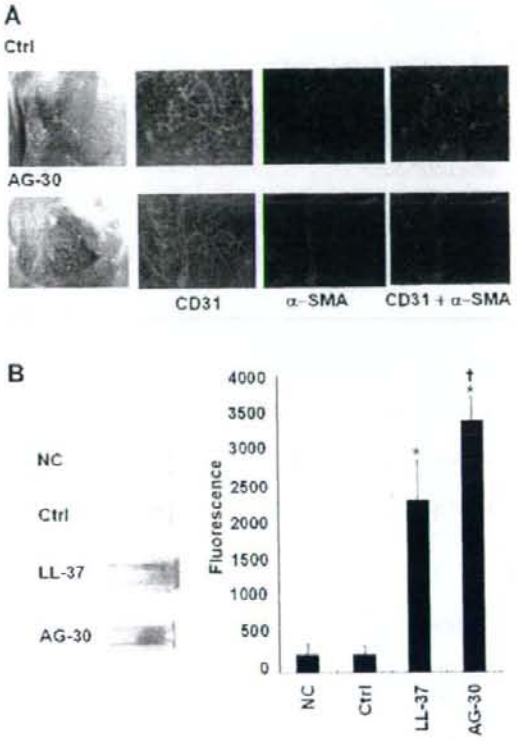

Fig. 3 Effect of AG-30 peptide on *in vivo* angiogenesis evaluated by Matrigel plug assay and directed *in vivo* angiogenesis assay (DIVAA). (**A**) Representative pictures of the Matrigel with AG-30 peptide or control peptide (10 μg/ml). Matrigel plugs were stained with anti-CD31 antibody (green) or anti-α-smooth muscle antibody (red), and capillary like structures were photographed ×100 magnification) under a fluorescent microscope. (**B**) Left panel shows that representative pictures of angioreactors implanted in mice, and the right panel shows the quantification of FITC-lectin positive cells that were treated with control peptide (10 μg/ml), LL-37 (10 μg/ml), AG-30 (10 μg/ml) or no treatment (NC). *$P < 0.05$ *versus* NC, †$P < 0.05$ *versus* Ctrl, ‡$P < 0.05$ *versus* LL-37. $n = 3$–4 per group.

Discussion

The present study demonstrated that a novel small peptide, AG-30, induced angiogenesis by promoting the expression of diverse angiogenic molecules. AG-30 was predicted to belong to a family of antimicrobial peptides that function to protect the host organisms against a large variety of invading pathogens [4–6]. These peptides are usually highly amphipathic molecules with hydrophobic and hydrophilic moieties segregating into distinct domains on the molecule surface.

In response to a bacterial membrane, AG-30 transforms to an α-helix structure and disrupts the membrane *via* a lytic effect. By contrast, the eucaryotic membrane does not induce a change in AG-30 structure change into an α-helix. Cholesterol, which is an essential component in the eucaryotic cell membrane, prevents self-damage of endogenous antimicrobial peptides [24]. This differential phenomenon underlies

Table 2 Cluster analysis using GeneSpring software to detect a twofold increased or decreased in gene expression at 72 hrs after AG-30 treatment

	6 hrs	24 hrs	72 hrs	
Angiopoietin 2	1.03	2.18	8.52	NM_001147
Angiopoietin-like 4, transcript variant	0.80	1.64	5.46	NM_139314
Interleukin 8	1.00	1.45	3.92	NM_000584
Jagged 1	1.73	1.31	3.90	NM_000214
Epiregulin	1.27	1.72	2.45	NM_001432
Vascular endothelial growth factor	1.36	0.87	2.07	NM_003376
Insulin-like growth factor	0.85	1.17	2.07	NM_00061
Neuropilin-1 soluble isoform 11	0.15	0.21	0.20	AF280547

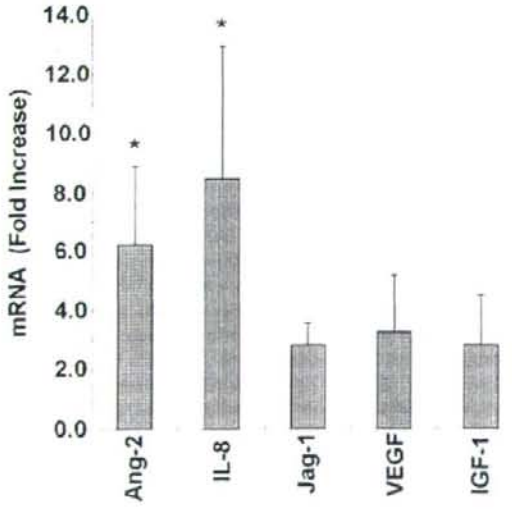

Fig. 4 Real-time quantitative reverse transcriptase polymerase chain reaction of angiopoietin-2 (Ang-2), Interleukin-8 (IL-8), Jagged 1 (Jag-1), vascular endothelial growth factor (VEGF) and insulin-like growth factor-1 (IGF-1) transcripts in HAEC at 72 hrs after treatment with AG-30. Results are expressed as fold-increase relative to the non-stimulants for copy numbers of each mRNA. *$P < 0.05$ *versus* Ctrl. $n = 3$ per group.

the ability of AG-30 to kill bacteria while simultaneously promoting endothelial cell growth. Defensins and cathelicidin families are well known as antimicrobial peptides, which are related to angiogenesis. Defensin contains 6–8 cysteine residues that form characteristic disulfide bridge, and shows β-sheet structure [25], which may be different from that of AG-30. In antimicrobial properties, both peptides can cover the similar broad spectrum, however AG-30, but not defensin, can directly induce angiogenesis. Moreover, defensin may induce apoptosis of human umbilical vein endothelial cell (HUVEC) and inhibits new capillary formation [26]. Human cathelicidin LL-37, on the other hand, is a peptide which has both antimicrobial and angiogenic effects [25]. In the present study, AG-30-stimulated EC growth, cell migration, tube formation and *in vivo* arteriogenesis was more potent than LL-37. LL-37-mediated angiogenesis is dependent on stimulation of a G-protein-coupled receptor that is upstream of the PLC-γ/PKC/NFkB, ERK-1 and 2 MAPK, and the PI3K/Akt pathways. Another porcine cathelicidin peptide, PR-39, appears to affect angiogenesis by inhibiting the ubiquitin-proteasome-dependent degradation of HIF-1α [10]. In our study, microarray analysis demonstrated that AG-30 induced increases in IGF-1, IL-8, JAG1, CCL2, CXCR2 or Ang-2 expression, all of which may independently induce angiogenesis [27–29]. For example, IL-8 is a potent chemotactic cytokine that

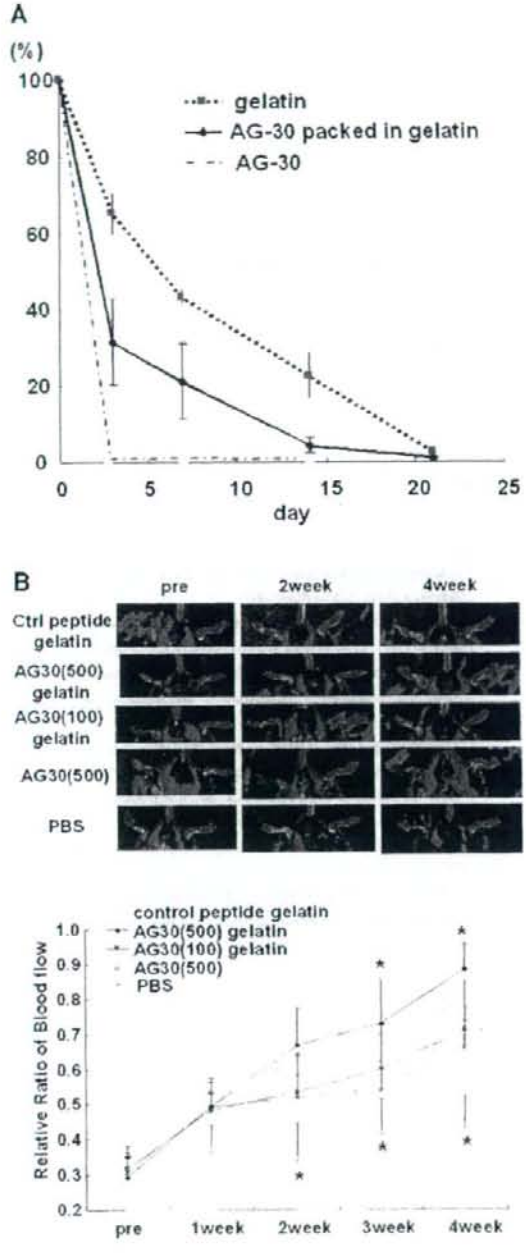

Fig. 5 Angiogenic effect of AG-30 in mouse ischaemic hind limb model. (**A**) Slow release profile of ^{125}I-labelled AG-30 with/without gelatin microspheres or ^{125}I-labelled gelatin at 3, 7, 14 and 21 day. (**B**) Evaluation of angiogenic effect by measuring mouse hind limb blood flow at pre-treatment (pre), 1, 2, 3 and 4 week. Ischaemic hind limb mouse were treated with gelatin/AG-30 (500 μg or 100 μg), gelatin/control peptide (500 μg), only AG-30 (500 μg) or PBS. Upper panel shows representative pictures of LDI images of hind limb blood flow at pre-, 2 and 4 weeks after treatment. *$P < 0.05$ versus control peptide gelatin. (**C**) Evaluation of capillary density of the AG-30-treated ischaemic hind limb. Upper panel shows representative photomicrographs (×400) of tissue immunostained with anti-CD31 antibody. Lower panel shows number of capillary per field. *$P < 0.05$ versus control peptide gelatin. $n = 5$–8 per group.

induces migration during angiogenesis [30] and its expression is regulated by NF-κB. Jagged-1 is a ligand of Notch signalling that regulates embryonic patterning and binary cell fate decisions and plays a critical role in mammalian embryogenesis and vascular development [31]. Although the exact mechanism is unclear, AG-30 could potentially act on several key molecules to regulate gene expression *via* autocrine or paracrine effects, thereby resulting in angiogenesis or vasculogenesis.

The effect of AG-30 on up-regulation of angiogenic genes appeared to be much slower than that of typical cell surface receptor-mediated processes. In fact, the AG-30-induced up-regulation of angiogenic genes was time-dependent and was maintained for at least 72 hrs. Of importance, we found that AG-30 was present in the nucleus at 24 or 48 hrs after treatment, which is a unique phenomenon when compared with other microbial peptides. Thus, AG-30 may enter the cytoplasm and nucleus in a sequential fashion to ultimately interact directly with transcription factors to regulate gene expression. We speculate that the ability of AG-30 to enter intracellular compartments may be cell type-dependent.

A slow-release system was used to stabilizing AG-30, as naked AG-30 peptide is very unstable and is easily degraded by proteases *in vivo*. As shown in Figure 4A, gelatin microspheres enabled the slow release of AG-30 in muscle over a period of 2 weeks in response to a single injection. One unique advantage of gelatin is its variable electrical nature (produced by altering the processing method of collagen) [32] that can be used to change its degradation rate or to modulate the physicochemical interactions between the drug and gelatin molecules [33]. The present study developed a suitable slow release system for AG-30 that resulted in therapeutic angiogenesis in a mouse ischaemic hind limb model. The release of AG-30 is driven by enzymatic degradation of carrier gelatin microspheres. Previous studies have reported the absence of inflammation, macrophage accumulation and granuloma formation around the injected site of cationized gelatin microspheres and that the degree of inflammatory reaction was dependent on the type and size of the particle [34]. Moreover, gelatin itself has been used for medical applications, and its biosafety has been proved through its extensive clinical use in surgical biomaterials. Thus, the use of this system may allow the application of AG-30 in various clinical conditions.

In summary, the present study identified a unique angiogenic and antimicrobial peptide, AG-30, with potential clinical applications. However, since small peptides are typically not stable *in vivo*, development of a drug delivery system to establish slow release of this peptide would be required for clinical utility.

Acknowledgements

We would like to thank all members of the Gene Therapy Science laboratory for critical discussion during the course of this work.

References

1. **Lalich M, McNeel DG, Wilding G, Liu G.** Endothelin receptor antagonists in cancer therapy. *Cancer Invest.* 2007; 25: 785–94.
2. **Jackson DC, Purcell AW, Fitzmaurice CJ, Zeng W, Hart DN.** The central role played by peptides in the immune response and the design of peptide-based vaccines against infectious diseases and cancer. *Curr Drug Targets.* 2002; 3: 175–96.
3. **Groneberg DA, Rabe KF, Fischer A.** Novel concepts of neuropeptide-based drug therapy: vasoactive intestinal polypeptide and its receptors. *Eur J Pharmacol.* 2006; 533: 182–94.
4. **Ganz T.** Defensins and host defense. *Science.* 1999; 286: 420–1.
5. **Steiner H, Hultmark D, Engstrom A, Bennich H, Boman HG.** Sequence and specificity of two antibacterial proteins involved in insect immunity. *Nature.* 1981; 292: 246–8.
6. **Izadpanah A, Gallo RL.** Antimicrobial peptides. *J Am Acad Dermatol.* 2005; 52: 381–90; quiz 91–2.
7. **Zasloff M.** Antimicrobial peptides of multicellular organisms. *Nature.* 2002; 415: 389–95.
8. **Zasloff M.** Antimicrobial peptides in health and disease. *N Engl J Med.* 2002; 347: 1199–200.
9. **Zasloff M.** Innate immunity, antimicrobial peptides, and protection of the oral cavity. *Lancet.* 2002; 360: 1116–7.
10. **Li J, Post M, Volk R, Gao Y, Li M, Metais C, Sato K, Tsai J, Aird W, Rosenberg RD, Hampton TG, Sellke F, Carmeliet P, Simons M.** PR39, a peptide regulator of angiogenesis. *Nat Med.* 2000; 6: 49–55.

11. **Larrick JW, Hirata M, Zhong J, Wright SC.** Antimicrobial activity of human CAP18 peptides. *Immunotechnology.* 1995; 1: 65–72.
12. **Koczulla R, von Degenfeld G, Kupatt C, Krotz F, Zahler S, Gloe T, Issbrucker K, Unterberger P, Zaiou M, Lebherz C, Karl A, Raake P, Pfosser A, Boekstegers P, Welsch U, Hiemstra PS, Vogelmeier C, Gallo RL, Clauss M, Bals R.** An angiogenic role for the human peptide antibiotic LL-37/hCAP-18. *J Clin Invest.* 2003; 111: 1665–72.
13. **Nishikawa T, Nakagami H, Matsuki A, Maeda A, Yo CY, Harada T, Morishita R, Tamai K, Kaneda Y.** Development of high-throughput functional screening of therapeutic genes, using a hemagglutinating virus of Japan envelope vector. *Hum Gene Ther.* 2006; 17: 470–5.
14. **Hunter HN, Jing W, Schibli DJ, Trinh T, Park IY, Kim SC, Vogel HJ.** The interactions of antimicrobial peptides derived from lysozyme with model membrane systems. *Biochim Biophys Acta.* 2005; 1668: 175–89.
15. **Pearson RD, Steigbigel RT, Davis HT, Chapman SW.** Method of reliable determination of minimal lethal antibiotic concentrations. *Antimicrob Agents Chemother.* 1980; 18: 699–708.
16. **Nakagami H, Morishita R, Yamamoto K, Taniyama Y, Aoki M, Matsumoto K, Nakamura T, Kaneda Y, Horiuchi M, Ogihara T.** Mitogenic and antiapoptotic actions of hepatocyte growth factor through ERK, STAT3, and AKT in endothelial cells. *Hypertension.* 2001; 37: 581–6.
17. **Rikitake Y, Hirata K, Kawashima S, Ozaki M, Takahashi T, Ogawa W, Inoue N, Yokoyama M.** Involvement of endothelial nitric oxide in sphingosine-1-phosphate-induced angiogenesis. *Arterioscler Thromb Vasc Biol.* 2002; 22: 108–14.
18. **De Y, Chen Q, Schmidt AP, Anderson GM, Wang JM, Wooters J, Oppenheim JJ, Chertov O.** LL-37, the neutrophil granule- and epithelial cell-derived cathelicidin, utilizes formyl peptide receptor-like 1 (FPRL1) as a receptor to chemoattract human peripheral blood neutrophils, monocytes, and T cells. *J Exp Med.* 2000; 192: 1069–74.
19. **Fukunaka Y, Iwanaga K, Morimoto K, Kakemi M, Tabata Y.** Controlled release of plasmid DNA from cationized gelatin hydrogels based on hydrogel degradation. *J Control Release.* 2002; 80: 333–43.
20. **Bolton AE, Hunter WM.** The labelling of proteins to high specific radioactivities by conjugation to a 125I-containing acylating agent. *Biochem J.* 1973; 133: 529–39.
21. **Nakagami H, Maeda K, Morishita R, Iguchi S, Nishikawa T, Takami Y, Kikuchi Y, Saito Y, Tamai K, Ogihara T, Kaneda Y.** Novel autologous cell therapy in ischemic limb disease through growth factor secretion by cultured adipose tissue-derived stromal cells. *Arterioscler Thromb Vasc Biol.* 2005; 25: 2542–7.
22. **Gaboriaud C, Bissery V, Benchetrit T, Mornon JP.** Hydrophobic cluster analysis: an efficient new way to compare and analyse amino acid sequences. *FEBS Lett.* 1987; 224: 149–55.
23. **Rikitake Y, Kawashima S, Yamashita T, Ueyama T, Ishido S, Hotta H, Hirata K, Yokoyama M.** Lysophosphatidylcholine inhibits endothelial cell migration and proliferation via inhibition of the extracellular signal-regulated kinase pathway. *Arterioscler Thromb Vasc Biol.* 2000; 20: 1006–12.
24. **Steiner H, Andreu D, Merrifield RB.** Binding and action of cecropin and cecropin analogues: antibacterial peptides from insects. *Biochim Biophys Acta.* 1988; 939: 260–6.
25. **Kougias P, Chai H, Lin PH, Yao Q, Lumsden AB, Chen C.** Defensins and cathelicidins: neutrophil peptides with roles in inflammation, hyperlipidemia and atherosclerosis. *J Cell Mol Med.* 2005; 9: 3–10.
26. **Chavakis T, Cines DB, Rhee JS, Liang OD, Schubert U, Hammes HP, Higazi AA, Nawroth PP, Preissner KT, Bdeir K.** Regulation of neovascularization by human neutrophil peptides (alpha-defensins): a link between inflammation and angiogenesis. *FASEB J.* 2004; 18: 1306–8.
27. **Smith LE, Shen W, Perruzzi C, Soker S, Kinose F, Xu X, Robinson G, Driver S, Bischoff J, Zhang B, Schaeffer JM, Senger DR.** Regulation of vascular endothelial growth factor-dependent retinal neovascularization by insulin-like growth factor-1 receptor. *Nat Med.* 1999; 5: 1390–5.
28. **Semenza GL.** HIF-1: mediator of physiological and pathophysiological responses to hypoxia. *J Appl Physiol.* 2000; 88: 1474–80.
29. **Rabinovsky ED, Draghia-Akli R.** Insulin-like growth factor I plasmid therapy promotes *in vivo* angiogenesis. *Mol Ther.* 2004; 9: 46–55.
30. **Koch AE, Polverini PJ, Kunkel SL, Harlow LA, DiPietro LA, Elner VM, Elner SG, Strieter RM.** Interleukin-8 as a macrophage-derived mediator of angiogenesis. *Science.* 1992; 258: 1798–801.
31. **Limbourg FP, Takeshita K, Radtke F, Bronson RT, Chin MT, Liao JK.** Essential role of endothelial Notch1 in angiogenesis. *Circulation.* 2005; 111: 1826–32.
32. **Veis A.** The physical chemistry of gelatin. *Int Rev Connect Tissue Res.* 1965; 3: 113–200.
33. **Ikada Y, Tabata Y.** Protein release from gelatin matrices. *Adv Drug Deliv Rev.* 1998; 31: 287–301.

Journal of Dermatological Science (2008) 51, 45–51

ELSEVIER

Journal of Dermatological SCIENCE

www.intl.elsevierhealth.com/journals/jods

Calcineurin/NFAT-dependent regulation of 230-kDa bullous pemphigoid antigen (BPAG1) gene expression in normal human epidermal keratinocytes

Takayuki Aizu [a], Katsuto Tamai [a,b], Hajime Nakano [a,*], Daiki Rokunohe [a], Yuka Toyomaki [a], Jouni Uitto [c], Daisuke Sawamura [a]

[a] *Department of Dermatology, Hirosaki University School of Medicine, 5 Zaifu-cho, Hirosaki 036-8562, Japan*
[b] *Division of Gene Therapy Science, Osaka University School of Medicine, 2-2 Yamadaoka, Suita-shi, Osaka 565-0871, Japan*
[c] *Department of Dermatology and Cutaneous Biology, Jefferson Medical College, Thomas Jefferson University, 233 South 10th Street, 450 BLSB, Philadelphia, PA, United States*

Received 21 February 2007; received in revised form 14 January 2008; accepted 28 January 2008

KEYWORDS
BPAG1;
Cyclosporin A;
Calcineurin;
NFAT

Summary

Background and objective: Cyclosporin A (CsA) is utilized widely for treatment of inflammatory skin diseases, such as psoriasis vulgaris. The therapeutic effects of CsA are thought to be mediated by its immunosuppressive action on infiltrating lymphocytes in the lesional skin. CsA also inhibits epidermal keratinocyte proliferation, suggesting a direct biological action on keratinocytes. Here we tested the hypothesis that CsA can modulate the expression of the nuclear factor of activated T-cell (NFAT) in epidermal keratinocytes. We also investigated whether the keratinocyte-specific gene expression is modified by CsA through NFAT activity in association with differentiation induction.

Methods: RT-PCR was performed using total RNAs extracted from cultured normal human epidermal keratinocytes (NHEK), normal human dermal fibroblasts (NHDF), and normal human epidermal melanocytes (NHEM) for detecting NFAT isomolecules. Transient transfections of NHEK with a 230-kDa bullous pemphigoid antigen (BPAG1) promoter/luciferase reporter gene and the luciferase assay were conducted for examining the effect of CsA on the promoter activity of the BPAG1 gene. Electrophoretic gel mobility shift assays (EMSA) with probes containing NFAT consensus

* Corresponding author. Tel.: +81 172 39 5087; fax: +81 172 37 6060.
E-mail address: hnakano@cc.hirosaki-u.ac.jp (H. Nakano).

doi:10.1016/j.jdermsci.2008.01.006

sequences for analyzing the binding activities of the nuclear proteins extracted from NHEK.

Results: RT-PCR revealed expression of all of the five isoforms of NFAT in the cell lines examined. The mRNA expression levels of NFAT1, NFAT2, BPAG1, and involucrin were downregulated by CsA treatment in NHEK. The luciferase assay indicated suppression of the promoter activity by CsA. EMSA with NFAT consensus probes identified in the BPAG1 promoter region demonstrated specific binding activity in the nuclear proteins of epidermal keratinocytes.

Conclusion: As reported previously, our results indicate that epidermal keratinocytes possess calcineurin/NFAT system, which is suppressed by CsA. In addition, the data suggest that CsA can downregulate the BPAG1 gene expression perhaps via the NFAT consensus *cis*-elements in the BPAG1 promoter region. Such transcriptional regulatory system might be involved in the regulation of keratinocyte differentiation and proliferation.

1. Introduction

Disorganized expression of inflammatory cytokines, such as interleukin (IL)-2, IL-4, IL-6, and IL-8 in infiltrating lymphocytes is thought to play a critical role in the pathogenesis of inflammatory skin diseases, such as psoriasis vulgaris, i.e. these cytokines induce aberrant growth and differentiation of epidermal keratinocytes. One of the major regulators of the expression of these inflammatory cytokines is the nuclear factor of activated T-cell (NFAT). NFATs constitute a family of five members of nuclear proteins, NFAT1/NFATp, NFAT2/NFATc, NFAT3, NFAT4/NFATx, and NFAT5, sharing a common primary structure. Each NFAT protein is extensively expressed in immune cells, although recent studies have suggested a wider distribution of NFATs in non-immune cells [1]. When activated by a rise in intracellular calcium, the calcium/calmodulin-dependent phosphatase calcineurin dephosphorylates NFAT, resulting in exposure of the nuclear localizing signal of NFAT, allowing its import into the nucleus and transcriptional activation of specific genes harbouring NFAT-responsive elements [1].

Cyclosporin A (CsA) is an immunosuppressive drug, which in T cells specifically binds to calcineurin and inhibits its phosphatase activity, consequently blocking the nuclear translocation of NFAT [1]. The expression levels of cytokine genes regulated by NFATs are reduced following treatment with CsA, i.e., CsA is immunosuppressive by acting on lymphocytes. These biopharmacological characteristics were delineated mostly in cells of immune systems. On the other hand, CsA has been demonstrated to modulate the biological functions in other cell types. It has been reported that growth of epidermal keratinocytes is inhibited by CsA treatment [2]. Moreover, several lines of experiments have demonstrated that calcineurin/NFAT activity is involved in keratinocyte growth/differentiation [3–5] and in control of the hair growth in vivo [6].

The present study was designed to test the hypothesis that CsA can modulate the expression of NFATs in epidermal keratinocytes. For this purpose, we examined the expression of NFATs in cultured normal human epidermal keratinocytes in the presence of various concentrations of CsA. We also investigated whether NFATs are involved in the transcriptional regulation of the 230-kDa bullous pemphigoid antigen (BPAG1) gene, a marker of undifferentiated, proliferating keratinocytes [7].

2. Materials and methods

2.1. Cell cultures

Normal human epidermal keratinocytes (NHEK) (Clonetics, San Diego, CA) were cultured in serum-free keratinocyte growth medium (KGM) (Clonetics), containing 0.03 mM calcium, epidermal growth factor (0.1 mg ml^{-1}), bovine pituitary extract (0.1 mg ml^{-1}), insulin (0.5 mg ml^{-1}), and hydrocortisone (0.5 mg ml^{-1}) at 37 °C under 5% CO_2–95% air. Cultures were passaged by trypsinization and studied in passage 2. In some experiments, CsA (a gift from Novartis, Switzerland) was added to the medium in final concentrations of 10^{-6}, 10^{-7}, or 10^{-8} M. Normal human dermal fibroblasts (NHDF) were cultured in minimum essential medium (MEM) (Gibco BRL, Gaithersburg, MD) with 10% FBS at 37 °C under 5% CO_2–95% air. Normal human epidermal melanocytes (NHEM) (Cascade Biologics, Portland, OR, USA) were maintained in medium 254 (Cascade Biologics) supplemented with recombinant bFGF (3 ng ml^{-1}), insulin (5 μg ml^{-1}), hydrocortisone (0.18 μg ml^{-1}), transferrin (5 μg ml^{-1}), heparin (3 μg ml^{-1}), phorbol-12-myristate-13-acet-

ate (PMA) (10 ng ml^{-1}), 0.2% (v/v) bovine pituitary extract (BPE), and 0.5% (v/v) FBS at 37 °C under 5% CO_2–95% air.

2.2. Reverse transcription-polymerase chain reaction

Total RNA was extracted using RNeasy Total RNA System (Qiagen, Hilden, Germany). cDNA was prepared with LA PCR kit (AMV) Ver. 1.1 (Takara Shuzo Co., Tokyo, Japan) using 0.5 mg of total RNA as template. Appropriate primers for PCR were designed based on cDNA sequences of NFAT1, NFAT2, NFAT3, NFAT4, NFAT5, BPAG1, involucrin, and glyceraldehyde-3-phosphate dehydrogenase (GAPDH), by computer program analysis. Sequences of these primers are shown in Table 1. After electrophoresis on 1% agarose gel, each band was quantified by densitometry and corrected for the levels of GAPDH in the same samples. Data are expressed as means ± S.D. of three independent experiments.

2.3. Protein extraction and western analysis

Protein extraction and western analysis were performed as previously described with minor modifications [8]. Keratinocyte extracts were subjected to SDS-PAGE and electrophoretically transferred onto a nitrocellulose membrane. The membranes were blocked with 5% nonfat dry milk in TBS containing 0.1% Tween-20, probed with goat polyclonal antibodies against a peptide mapping near the C-terminus of human BPAG1 (Santa Cruz Biotechnology, Santa Cruz, CA, USA), and then allowed to react with rabbit anti-goat IgG antibody conjugated with horseradish peroxidase.

Table 1 Primer sequences used for RT-PCR

Gene	Primers
NFAT1	5′-GAATATGACCCCACTCTGAT-3′ (sense)
	5′-TTGGTGGGTGAGTAGTGGAT-3′ (antisense)
NFAT2	5′-CGGAAAGGAGAGACGGACAT-3′ (sense)
	5′-ATCTTCTTCCCGCCCACGAC-3′ (antisense)
NFAT3	5′-CTTGCGAAACTCCTTACCTA-3′ (sense)
	5′-ACATCACTCTGGGAAGGGAA-3′ (antisense)
NFAT4	5′-CTTTCAGTTCCTTCACCCTT-3′ (sense)
	5′-CAGGATGTCCCCCAGTAGAT-3′ (antisense)
NFAT5	5′-CAACAGAGCCAACAGTCCAT-3′ (sense)
	5′-CCTGCTGTGTGGTAGTTGTA-3′ (antisense)
BPAG1	5′-AGCAAAGGACGCATACTGAC-3′ (sense)
	5′-ATTTGGCTCTACTCCTGAAC-3′ (antisense)
GAPDH	5′-ACCACAGTCCATGCCATCAC-3′ (sense)
	5′-TCCACCACCCTGTTGCTGTA-3′ (antisense)

2.4. Transient transfection and luciferase assays

A plasmid pBP1.9luc, which contains the 1.9-kb promoter region from −1908 to −1 of the BPAG1 gene [9] in front of the luciferase reporter gene, was generated with a plasmid vector pGEM-luc3 (Promega, Madison, WI). The plasmid pBP1.9luc was then co-transfected with CMV-lacZ plasmid into NHEK using Mirus liposomal transfection reagent (PanVera Co., Madison, WI); 0.5 μg of each plasmid was used in the transfection of NHEK cultured on 6-cm dishes with KGM medium containing 0.03 mM calcium. After 6-h incubation, the medium was removed from dishes, and the cultures were further incubated for another 6–24 h in fresh KGM medium containing CsA at a final concentration of 10^{-6}, 10^{-7} or 10^{-8} M. After incubation, cells were rinsed twice in PBS, dissolved in 300 μl cell lysis reagent (Wako Pure Chemical Industries, Osaka, Japan) and harvested by scraping. Luciferase assays were performed by using luciferase assay system (PicaGene, Wako) and luminometer (Lumat LB9501, Berthold). Luciferase activity was measured in a mixture of 20 μl cell extract and 100 μl luminary base, and then normalized for the β-galactosidase activity derived from co-transfected CMV-lacZ plasmid. Data are expressed as means ± S.D. of three independent experiments in duplicate.

2.5. Electrophoretic gel mobility shift assays

NHEK were cultured in KGM at 37 °C and nuclear protein was extracted using the method described previously [10]. Search for NFAT consensus sequence in the BPAG1 gene promoter region by a homology search program DNASIS®Pro (Hitachi Software Engineering Co. Ltd., Tokyo, Japan) identified three canonical NFAT consensus sequences in the regions −299 to −291, −607 to −599, and −894 to −886, upstream from the transcription starting site (−1/+1) [9]. These regions were designated as BP-P, BP-M, and BP-D, respectively (Table 2). Double-stranded oligomer DNA probes labeled with ^{32}P were incubated with 5 μg of nuclear protein extract. The DNA-protein complexes were then subjected to polyacrylamide gel electrophoresis as described previously [11]. In the competition assays, unlabeled DNA probe was added to the incubation mixture in concentrations up to 100-times higher than the labeled probe. After 30-min incubation on ice, these samples were subjected to the gel shift assay.